STM JOURNALS

Journal of
Remote Sensing & GIS

https://journals.stmjournals.com/jorsg

ISSN: 2230-7990 (Online)
ISSN: 2321-421X (Print)
Volume 16, Issue 1, 2025
January–April
DOI (Journal): 10.37591/JoRSG

Research JoRSG

A Geospatial Analysis of Correlation Between Built-Up Area and Vegetation Coverage Using Google Earth Engine in Saint Martin Island, Bangladesh

Md. Jakir Hossain[1,*], Md. Munir Mahmud[2], Sheikh Tawhidul Islam[3]

Abstract

Background: *This study explores the complex interconnection between expanding human settlements and fluctuating plant life on the island of Saint Martin, Bangladesh, utilizing cutting-edge geospatial techniques through the open-source Google Earth Engine platform. The rapid population boom in Bangladesh and tourism-fueled development on Saint Martin Island stir serious worries about their ecological consequences.* ***Methods:*** *Remote sensing data sourced from Landsat 5 TM and Landsat 8 OLI/TIRS satellites between 1991 and 2022 were leveraged to dynamically calculate the Normalized Difference Vegetation Index and Normalized Difference Built-up Index, exposing variations over time. Regression investigation uncovers the relationship between urban density and green coverage by scrutinizing the change of Normalized Difference Built-up Index (NDBI) and Normalized Difference Vegetable Index (NDVI) within land use classifications. The methodology is transparently documented in appendices, ensuring accuracy and replicability.* ***Results:*** *A faint inverse link between NDVI and NDBI was found, implying construction has a minimal impact on greenery. Clear patterns emerge in-built zones examining NDBI values, with 1991 showing the highest urbanization levels. In 2022, findings indicated a moderate adverse connection between the plant index and development index. However, 1991, 2001, and 2011 saw a weak linear negative correlation, suggesting buildings marginally impact vegetation worth.* ***Conclusions:*** *This research enhances comprehension of urbanization's effects on plants, providing valuable insights for sustainable city planning and land management. The study spotlights Earth Engine's analytical prowess for geospatial inquiries across diverse settings.*

Keywords: Built-up, vegetation, NDVI, NDBI, correlation, geospatial analysis, Google Earth Engine (GEE), Saint Martin Island

***Author for Correspondence**
Md. Jakir Hossain
E-mail: jakirhossain.urpju45@gmail.com

[1]Student, Department of Remote Sensing and GIS, Jahangirnagar University, Dhaka, Bangladesh
[2]Assistant Professor, Department of Remote Sensing and GIS, Jahangirnagar University, Dhaka, Bangladesh
[3]Professor, Department of Remote Sensing and GIS, Jahangirnagar University, Dhaka, Bangladesh

Received Date: November 26, 2024
Accepted Date: December 10, 2024
Published Date: December 24, 2024

Citation: Md. Jakir Hossain, Md. Munir Mahmud, Sheikh Tawhidul Islam. A Geospatial Analysis of Correlation Between Built-Up Area and Vegetation Coverage Using Google Earth Engine in Saint Martin Island, Bangladesh. Journal of Remote Sensing & GIS. 2025; 16(1): 21–39p.

INTRODUCTION

Understanding the intricate expansion of cities and their impact on the delicate environment necessitates judicious mapping and multifaceted analysis of sprawling urban regions and fluctuating vegetation coverage. In less developed nations like Bangladesh, the precipitous increase in population has prompted a burgeoning demand for fundamental necessities such as housing, educational institutions, medical facilities, transportation, and leisure spaces. Comparable to ecologists meticulously monitoring transformations, the proliferation of cities often encroaches on agricultural land and diverse greenery, inevitably leading to notable repercussions for the balance between the delicate environment and fragile natural ecosystems.

Furthermore, renowned tourist destinations, such as the scenic coral island of Saint Martin in Bangladesh, may experience comparable effects prompted by the growth driven by burgeoning tourism, potentially resulting in the deterioration of the unique flora on this island, as highlighted by several studies on this topic [1–3].

Researchers have developed various analytical techniques to investigate urban growth dynamics over time. Metrics such as the Urban Index, Normalized Difference Bareness Index, and Bare Soil Index leverage remote sensing datasets and spectral signatures to categorize land use classifications. These indices provide valuable insights into intricate patterns of urban expansion. The commonly used Normalized Difference Built-up Index (NDBI) scores range from negative to positive. Interpreting these values depends on contextualizing them within the characteristics of the study area and the parameters of the analysis. Generally, higher positive NDBI readings indicate landscapes with a greater proportion of constructed or urbanized surfaces within the scene. Conversely, lower or negative NDBI values typically represent places with less development, such as vegetated regions or bodies of water. A proper understanding of index values and their distribution across the landscape under examination is paramount to drawing meaningful conclusions regarding urban growth processes.

Remote sensing technologies are often employed to gauge and track vegetable situations through vegetation indications, such as the Enhanced Vegetable Index (EVI) and Normalized Difference Vegetable Index (NDVI) [4]. In semi-arid environments, NDVI is commonly used to evaluate plant productivity and degree of dampness. NDVI plays a pivotal role in monitoring plant territories and constructing indices, as it responds to the red-impacted zone with high absorption. The indices are derived from combinations of spectral bands that seize the exceptional qualities of plant existence. This equipment is used for tracking cropping patterns, phenology, vegetable types, classifications, and deriving vegetative biophysical constraints. On the NDVI scale, there was a variety from -1 to +1. Negative values indicate water bodies, snow, barren floors, and city areas, while optimistic values are linked to agricultural land, crops, pastures, and inexperienced vegetation. The NDVI is widely recognized for its capacity to reduce the effects of topographic influences, cloud shadows, changing light angles, and climatic stipulations. The index is correct, dependable, and easy to apply for mapping crops and agricultural land in tropical regions [5].

Our objective was to explore the relationship between city development and vegetation in Saint Martin Island, Bangladesh. To accomplish this, we will employ state-of-the-art geospatial techniques with the assistance of Google Earth Engine. While there has been extensive research on geospatial analysis, no one has specifically investigated this relationship on Saint Martin Island. An intensive research venture investigated changes within the coastline from 1974 to 2021 using a mixture of geospatial and statistical strategies, including Data Structures and Algorithms (DSAs), Normalized Difference Water Index, and Tasseled Cap Transformation. As part of the observation, the Kalman Filter Model was used to predict the destiny charges of erosion and accretion.

A comprehensive study investigating the impacts of vegetation indicators and atmospheric conditions in Bangladesh was conducted using the geospatial analysis of satellite imagery. This research incorporated Moderate Resolution Imaging Spectroradiometer (MODIS) datasets from Google Earth Engine to examine trends from 2000 to 2019, finding a steady rise in the NDVI that correlated with environmental changes over time. Separately, the effect of monsoon flooding on land surface temperature and plant life in remote northeastern regions was explored by assessing the links between climatic elements and greenery. However, this analysis centered on natural influences alone, without delving into connections between urban growth patterns and diminishing natural land on the tiny island of Saint Martin, as reported elsewhere. Additional location-specific examinations of the relationship between anthropic development and biodiversity losses in delicate coastal zones are still needed to fully grasp multiplier threats and help safeguard endangered ecosystems.

Google Earth Engine-based studies have investigated the relationship between NDVI and NDBI. Pamungkas investigated land cover changes and impacts on NDVI and Land Surface Temperature (LST) in the Muzaffarpur district, Bihar, India [6]. This study created a data plant index from the Google Earth Engine platform, which found that NDVI has a strong relationship with water pH in Lembar Bay [6]. Arias and Celemín analyzed changes in the vegetated surface of the central region of Santiago del Estero, Argentina, and its urban population density using data acquired from satellites [7]. Correlation analysis revealed a strong negative NDVI-Urban Index (UI) correlation. Khan [8], in their study, examined the relationship between NDVI and the LST of Maharashtra, Central India. The investigation revealed a significant negative correlation between NDVI and LST. Unfortunately, no applicable research paper has been found that applies to the relationship between urban development and vegetation quantities on Saint Martin Island. This study aims to provide insights into the intricate interactions between urban development and vegetation sustainability on the island by examining this relationship. This will be done through the deep power of Google Earth Engine [9, 10].

The use of vegetation and built-up indices based on remote sensing techniques has been widely used in previous studies. For many ecologists, NDVI is an essential indicator of vegetation and has been used in association analyses with NDVI-NDBI, LST-NDVI, and NDVI-NDWI relationships. Such studies have effectively provided useful information on the interactions between land use and environmental changes through a synergy of vegetation and built-up indices. Relying on available knowledge, our study assesses the relationship between NDVI and NDBI over Saint Martin Island, Bangladesh, for the years 1991–2022. By studying the correlation between urban land use and vegetative cover change on the island, the objectives of this study were to gain insight into how both impervious land areas and plant morphology have varied over time. This study will help to assess the impact of tourism increase on vegetation cover and inform future planning strategies to maintain sustainable land use practices in response to this growing population on Saint Martin Island.

AIMS AND OBJECTIVES

This study aims to perform a synoptic-scale geospatial analysis using Google Earth Engine (GEE) of urbanized areas to vegetation coverage on Saint Martin Island, Bangladesh. Based on this general goal, two specific objectives were defined.

- The spatial distribution patterns of the built-up areas and vegetation coverage across the island were investigated.
- We analyzed the correlation between built-up areas and vegetation coverage, and its significance in the study area.

METHODS

Study Area Profile

Saint Martin Island, referred to by natives as "Narikel Jinjira," consists of a mere three-square kilometer of land. Located in the northeastern region of the Bay of Bengal, approximately 9 km south of the tip off Cox's Bazar–Teknaf peninsula, this place is notable for being the southernmost point of Bangladesh. On the other hand, it is a small island, known as Chera Dwip, which is separated from the rest during high tide. Situated about 8 km offshore from the northwestern coast of Myanmar at the mouth of the Naf River [11], this coral island is a unique natural treasure within Bangladesh.

Saint Martin Island was previously joined to the Teknaf Peninsula. Over a long period of sinking, the southernmost end isolated itself as an island and was no longer part of the main continent. A map of the study area (Saint Martin Island, Bangladesh) is shown in Figure 1. As for the island, it was settled 250 years ago in the 18th Century by Arabian merchants who called it 'Jazira'. This island was named St. Martin Island by British rulers as a mark of respect to Mr. Martin, Deputy Commissioner of Chittagong at the time. This seems to be a strong factor in the selection since we do not know who the actual Arab settlers are, but probably there are saints among them. It is locally known as "Narikel Jinjira" or 'Coconut Island' and "Daruchini Dwip" or 'Cinnamon Island' [8]. Saint Martin Island is unique in its ecological setup, as it is the only true coral island in Bangladesh.

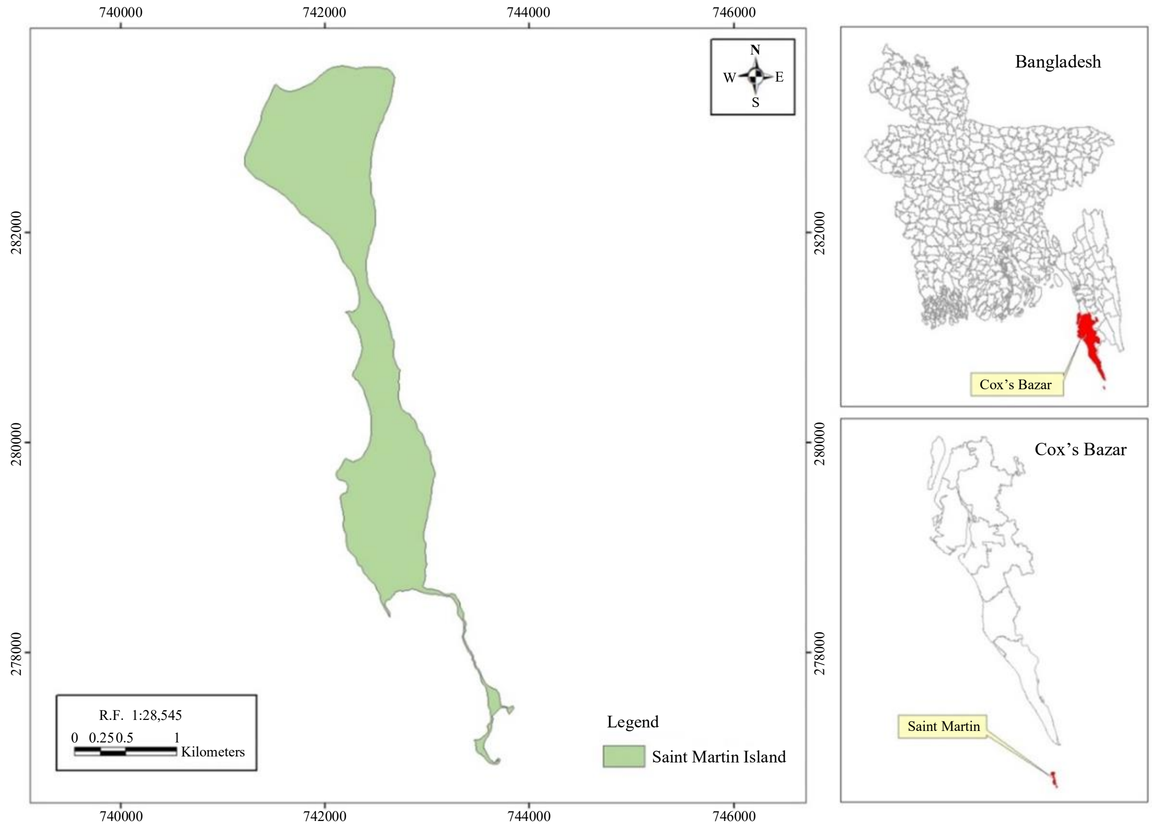

Figure 1. Study area map (Saint Martin Island, Bangladesh).

It comprises nine villages or areas within the Saint Martin's Union Parishad: Paschim Para (Western Neighborhood), Deil Para, Uttar Para (Northern Neighborhood), Majher Para (Middle Neighborhood), Purba Para (Eastern Neighborhood), Konar Para (Edge Neighourhood), Nazrulpara (Neighbourhod of Nazrul) [12] and Golachipa (literally "narrow neck") and Dakkhin Pada (Southern Neighborhood).

According to an ecologist, the island of Saint Martin pulls with almost 3,700 residents. Their diet primarily consists of fish, with rice and coconuts as staple crops. It is famous for the mass collection, drying, and shipment of algae to Myanmar. Between October and April, fishers from the surrounding area meet the island's makeshift wholesale market to sell their catch. However, key food items such as chicken and meat are imported from mainland Bangladesh and Myanmar. From the perspective of an ecologist, long-lasting structures are located far north, whereas farmland and temporal huts make up most of the central and southern regions [3, 12].

In particular, during the rainy season, people are stranded in the Bay of Bengal, where it is unsafe for shipping to ply to the mainland (Teknaf). There have been times before medical personnel were not immediately available on the island, even though there was a hospital. A study commissioned by the United Nations Development Programme(UNDP) and conducted by the Bangladesh Department of Environment found a variety of ecosystems on the island including coral reefs, mangroves, lagoons, and rocky areas. Saint Martin is home to all types of wildlife, including seaweed, corals, oysters, fish, birds, reptiles, and mammals. The island harbors diverse species such as those identified in 2010.

This neighboring region was designated a Marine Protected Area in 2022 because of its ecological importance. Important research led in 2021, by Paul et al. [8] showed that nine marine sponge species found on the island produced a plethora of bioactive compounds. Moreover, from these marine sponges, bacteria containing 15 genera and 31 species were recovered in this study. Of these, some have been found to be probiotic candidates [8, 13].

Tourists all over the world travel to Saint Martin Island. Today, eight ferry firms ply to the islands every day. Tourists show a clear trend that ecotourism and beach resorts can go to sustainable tourists and advance environment-friendly users. You can arrange trips directly from Chittagong or Cox's Bazar. The island's coral reef extends to the empty Chera Dwip, which is known to be covered with a low-green shrub. It is recommended to explore this area in the early morning and return by noon [8]; thus, all tourists should visit this region in the early hours of the day [5, 8].

Conservation efforts have also focused on the island's endangered turtle species and its endemic corals. Unfortunately, coral reef pieces are sometimes harvested and sold as souvenirs to tourists, affecting their conservation. Nesting turtles are also eaten, and light pollution on the beach distracts the hatchlings. You have got new species that have been discovered, but it is also at risk of being overexploited by the surrounding fish population. This means that fishermen must go out further for their catch. The island's existence relies on its coral foundation. If coral is punted out, there is also the potential for a hugely damaging loss of coastline through erosion. Over the last 40 years, more than 70 percent of Saint Martin Island's coral reef has been lost. This unfortunate trend has been caused by humans. However, as an ecologist would notice, Saint Martin Island is shaken by a high density of visitors. The land use patterns of the island are deteriorating because of the construction of tourism-recreational facilities [14].

Data Acquisition and Pre-Processing

Google Earth Engine is a cloud-based platform that redefines the way remote sensing processing is performed by offering numerous different algorithms to collect and analyze many types of geoscience data. GEE provides strong interaction and computation capabilities, making the work cycle easier by removing the need for downloading images, which ultimately makes GEE a better choice for workflows [15]. This revolutionary platform allows remote sensing scientists to focus less on processing and more on performing a deeper analysis, saving time and increasing productivity in geospatial science. The research is based on data obtained using remote sensing technology, specifically Landsat 5 TM for 1991, 2001, and 2011, as well as Landsat 8 OLI/TIRS for 2022. The data were obtained meticulously from the Google Earth Engine Cloud platform and cross-verified through the United States Geological Survey(USGS) web portal. All of them were in Tagged Image Files (TIF) format. This study, which analyzed images taken in January, February, and March with an emphasis on data quality, focused only on the dry season. The selection process was strict; thus, the cloud cover had to be minimal. Remote sensing images were projected onto the study wraps mapped by the Universal Transverse Mercator (UTM) projection framework [15, 16].

A single Landsat 8 and Landsat 5 scene were found (within WRS-2) within the data subset with the coordinates of path 135, row 046. Table 1 contains all the information required for the reference. The satellite images were then processed using integrated geospatial tools as part of the Google Earth Engine Platform. The last map base was created using the ArcGIS 10.8 environment in a certain complex process of image processing to ensure the accuracy and reliability of visual representation in the actual development prospect area. In addition, the shapefile of Saint Martin Island was retrieved from the Survey of Bangladesh (SOB) database. Because the satellite image contained data from both classes,

Table 1. Illustrate the data on acquired Landsat images from 1991, 2001, 2011, and 2022.

S.N.	Landsat name	Row/path	Acquisition date	Scene ID
1.	Landsat 8 (OLI/TIRS)	135/046	2/26/2022	LC09_L2SP_135046_20220226_20230426_02
2.	Landsat 5 (TM)	135/046	2/20/2011	LT05_L2SP_135046_20110220_20200823_02
3.	Landsat 5 (TM)	135/046	3/28/2001	LT05_L2SP_135046_20010328_20200906_02
4.	Landsat 5 (TM)	135/046	2/13/1991	LT05_L2SP_135046_19910213_20200915_02

Source: USGS

it was essential to use this instrument file for masking and isolating specific study areas from the rest of the satellite imagery, ensuring careful inspection of the target area under study.

NDVI and NDBI were computed from specified satellite images. The implementation of NDVI in utilizing remotely sensed data is an important step for mapping and monitoring vegetative regions and has become the basis for many studies [17, 18]. Its versatility is evidenced by the fact that it has been used for multiple applications including drought assessment, estimating crop yields, fire risk prediction, and global desertification mapping. NDVI is not only limited by climate and region but also by its excellent adaptability under different illumination conditions, surface slopes, faces, etc.

NDVI values range from -1 to 1, depending on the ratio of the relative digital number (DN) for both the near-infrared and red bands. Negative pixel values in this range represent features, such as rocks, clouds, snow, surface water, and bare land. Negative values, typically between 0.1 and 0.2, suggest vegetated areas, while the opposite is true for positive values. This value makes sense; however, these could also be affected by harvesting, so healthier canopies normally within 0.5 end up dropping down a fair bit. In contrast, areas of sparser vegetation typically have values between 0.2 and 0.5). Moderate vegetation is typically between 0.4 and 0.6. Values higher than 0.6 reveal the strongest concentration of green leaves. NDVI Calculation: There are equations for the calculation of NDVI for Landsat 8 OLI/TIRS (Equation (1)) and Landsat 5 TM (Equation (2)). Such equations are essential for rectifying NDVI values to obtain a clearer view of the vegetation landscape within the study area.

$$\mathrm{NDVI} = \mathrm{NIR\ (Band\ 5)} - \mathrm{Red\ (Band\ 4)}/\mathrm{NIR\ (Band\ 5)} + \mathrm{Red\ (Band\ 4)} \quad (1)$$

$$\mathrm{NDVI} = \mathrm{NIR\ (Band\ 4)} - \mathrm{Red\ (Band\ 3)}/\mathrm{NIR\ (Band\ 4)} + \mathrm{Red\ (Band\ 3)} \quad (2)$$

In contrast to the vegetation index NDVI, the NDBI was developed for analyzing, mapping, and monitoring built-up and settlement areas using remote sensing data. The NDVI is useful for extracting vegetation, whereas NDBI is used for the identification and extraction of urban areas and built-up settlements. For the initial analysis, NDBI values and their respective maps were obtained from accurate data collection using Landsat 8 OLI/TIRS data and Landsat 5 TM. The reflectance characteristics of urban covered areas differ in spectral dimensions from other developed categories. The NDBI values governed by (x1 = MIR and x2 = NIR) range from −1 to 1, in which higher value pointers indicate a low or high percentage of association with built-up areas within the landscape. We must mention that these regions show more reflection compared to the near-infrared (NIR) wavelength range of 0.76–0.90 µm [10]. For precise and accurate measurement of NDBI values using remote sensing, we used specific computational equations: Equation 03 for Landsat 8 OLI/TIRS [19] and equation variable available but cannot be extracted for Landsat 5 TM (2000) [18]. It is one of the equations used for the detection and mapping of developed and settled areas within the study area. This provides insight into age-old phenomena that shape urban development dynamics and settlement patterns, offering a great sense of their relationship in terms of evolutionary changes [19].

$$\mathrm{NDBI} = \mathrm{MIR\ (Band\ 6)} - \mathrm{NIR(Band\ 5)}/\mathrm{MIR\ (Band\ 6)} + \mathrm{NIR\ (Band\ 5)} \quad (3)$$

$$\mathrm{NDBI} = \mathrm{MIR\ (Band\ 5)} - \mathrm{NIR(Band\ 4)}/\mathrm{MIR\ (Band\ 5)} + \mathrm{NIR\ (Band\ 4)} \quad (4)$$

The overall methodology used in this study is illustrated in Figure 2. NDVI and NDBI were calculated using algorithms developed on the Google Earth Engine platform. This was followed by an evaluation of the relationship between these indices when programmed using JavaScript. We conducted an extensive evaluation to ensure the accuracy of the results. Finally, their investigation results had new layout maps that were much simpler to create using ArcGIS. A flow diagram is shown in Figure 2.

This study presents the output interface of the GEE and provides readers with a more detailed analysis in the appendix section. This section presents an in-depth exploration of the technical details and computation complexities behind the methodology in question, making it clear how it was possible to come up with a research result, such as the one carried out in this study.

Journal of Remote Sensing & GIS
Volume 16, Issue 1
ISSN: 2230-7990 (Online), ISSN: 2321-421X (Print)

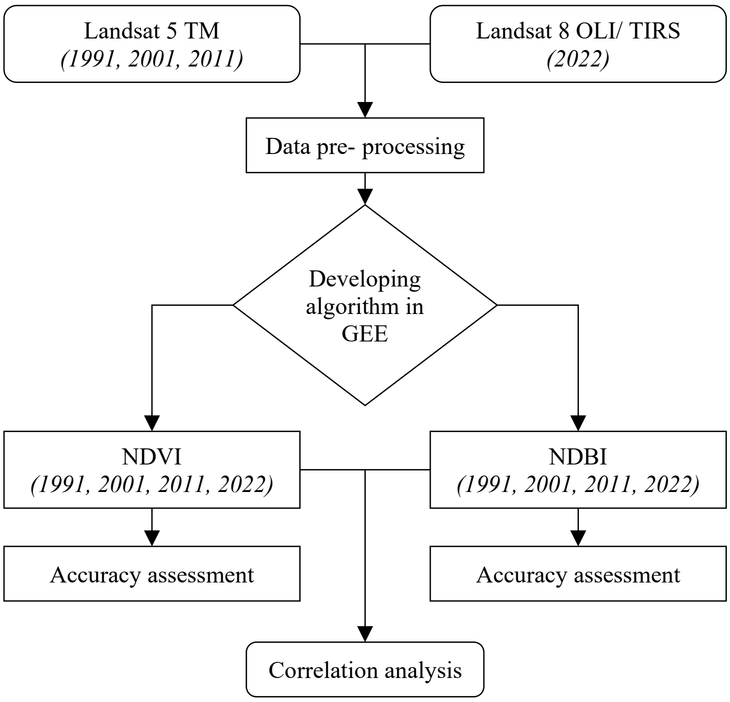

Figure 2. Methodology flow diagram.

Accuracy Assessment

The NDVI and NDBI indices, together with Landsat 8 and Landsat 5, were extracted from the study area and an accuracy assessment was performed. For example, the NDVI from Landsat 5 generally has an accuracy of 69.12% with a kappa coefficient of 0.589. In comparison, the Landsat 8 NDVI, with an overall accuracy of 76.83% and a kappa coefficient of 0.643, had higher precision. A stratified random sampling approach was used to assess the accuracy of the proposed NDBI method. In total, 50 samples from built-up and non-built-up areas were assessed. The results showed the applicability of the proposed NDBI method, where the total accuracy was reached (86.30% for Landsat 8 and 82.65% for Landsat 5). This remarkable accuracy further emphasizes the reliability and precision of the NDBI methodology for recognizing built-up areas from satellite images.

RESULTS

Vegetation Coverage and Built-Up Area Identification Using False Color Composite Map

This study analyzed satellite data from 1991, 2001, 2011, and 2022 to map changes in Saint Martin Island, Bangladesh over time. Four false color composite maps were created using spectral bands from the Landsat 5 and Landsat 8 satellites. These detailed images show the terrain of the island with varying shading. Built-up areas stand out when using an assigned color scheme. The near-infrared, shortwave infrared and visible blue bands were allocated to the red, green, and blue channels, respectively, to generate the maps.

This band combination facilitates the easy identification of lush greenery, appearing in rich son hues. Additionally, bodies of water are discernible because of the unique colors of ebony and azure. Urban settings emerge in an assortment of gray or ivory tones, depending on the development level and surrounding flora density. Figure 3 illustrates the island's landscape evolution over time. It traces alterations in vegetation and constructed areas, revealing their interconnected shifts over space and time.

Computation of Normalized Difference Vegetation Index

In Figure 4, we can see the NDVI values from several years of worth of images shown graphically. An NDVI of -0.375 was reported over non-vegetated areas such as expanses of open water, swaths of barren terrain, and expansive sandy regions in 1991, whereas an NDVI of 0.686 indicated substantial and robust plant cover across much of the landscape.

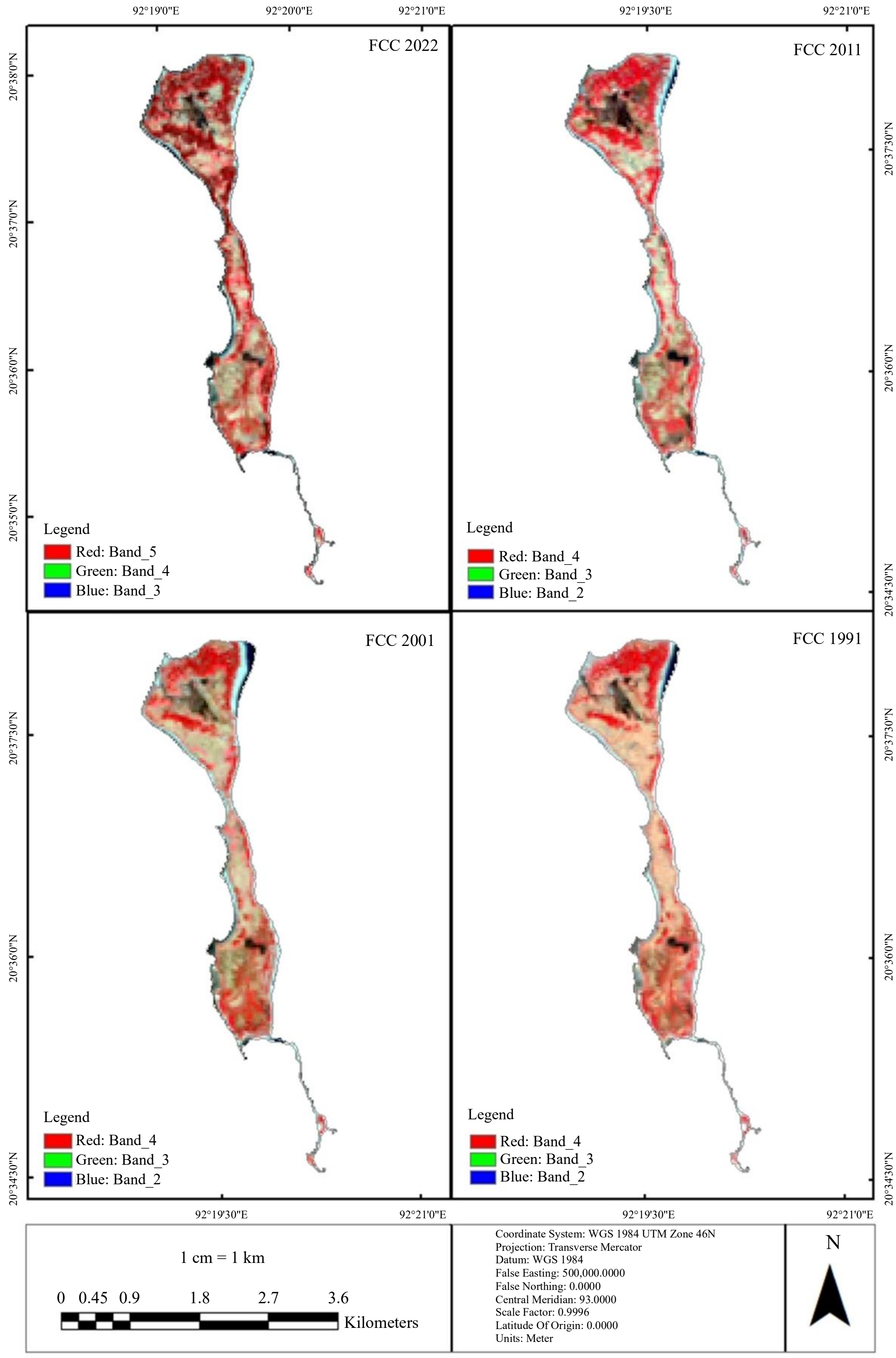

Figure 3. Vegetation and built-up area identification using false color composite from 1991 to 2022.

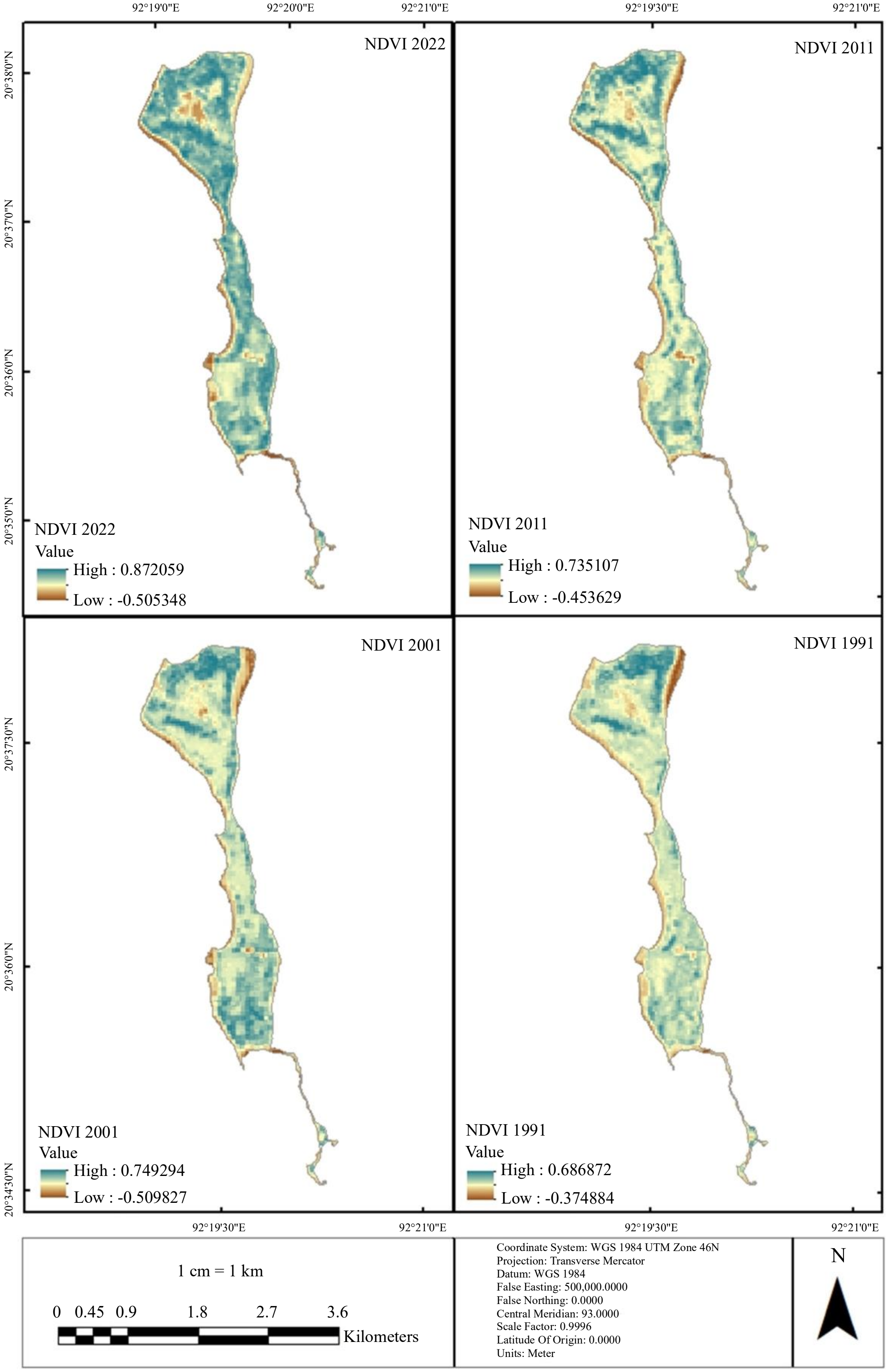

Figure 4. Represents NDVI of 1991, 2001, 2011, and 2022.

Moving ahead ten years to 2001, analysis of the NDVI images showed a maximum value of 0.749, signifying strong, dense, and verdant vegetation across wide stretches, and a low value of -0.509 in locales with little to no thinly scattered vegetation. 2011 was the year when the highest NDVI value peaked at 0.735, suggesting significant and widespread plant coverage across most of the island. In contrast, regions characterized by sparse sandy soil, arid conditions unfavorable for growth, and expanding urban development exhibited the lowest values of approximately -0.454.

When the NDVI levels ultimately hit their zenith in 2022, the highest figure ever documented was 0.872, mostly evident over normally arid and sandy terrain in the northern half of Saint Martin Island. On the other hand, locales demonstrating minimal vegetative cover were found to have the lowest NDVI, dipping to -0.505. Upon scrutinizing the NDVI values seen throughout the time from 1991 to 2022, a notable pattern emerged. The greatest NDVI readings in 2022 indicate a burgeoning plant canopy, which is especially visible across expansive agricultural fields. Satellite imagery from 1991 showed the lowest NDVI values, signifying comparatively reduced vegetative coverage during that earlier time. The dynamic fluctuations in plant density observed across the island over the decades are vividly depicted in this graphical display.

Computation of Normalized Difference Built-Up Index

The NDBI values obtained from the 1991 aerial photographs ranged from 0.302 to -0.545, as shown in Figure 5. These numbers pinpoint the most densely populated and least crowded locations of Saint Martin Island. A lower NDBI reading corresponds to areas such as water bodies and places affluent in flora, whereas a higher value indicates spots with a greater population thickness and less plant cover. Examining the snapshots from 2001, the NDBI values show a peak constructed region amounting to 0.277. In contrast, the study area recorded the lowest NDBI value of -0.968. This illustrates how different natural and vegetated places are from heavily congested metropolitan territories. Vegetation and Built-up Area Identification using false color composites from 1991 to 2022 are shown in Figure 3.

Regions categorized as hamlets, sandy terrain, and barren land had the greatest value, at 0.232, as per the 2011 NDBI photographs. On the other hand, areas with many crops, vegetation, and grasslands had minimum values, with an NDBI of -0.545. The NDVI of 1991, 2001, 2011, and 2022 is shown in Figure 4. The built-up index achieved a high of 0.260 and a low of -0.710 in 2022. Plants and bodies of water were the most typical locations where these values were observed. The NDBI for 1991, 2001, 2011, and 2022 is shown in Figure 5.

A clear trend became apparent when the NDBI values were compared from 1991 to 2022. In 1991, built-up regions reached their zenith, as the most intensive urbanization occurred during that time. By contrast, the images taken in 2022 revealed the lowest NDBI values, indicating that comparatively fewer urban areas existed in that year. Undeniably, the NDBI serves as a strong signal for differentiating built-up zones in satellite imagery. Table 2 provides a thorough synopsis of the NDVI and NDBI across the timeframe from 1991 to 2022 by aggregating their maximum and minimum values.

Table 2 shows the NDVI and NDBI figures for 1991, 2001, 2011, and 2022 on the island of Saint Martin. The assorted urban and greenery levels have emerged from examining the fluctuations in these values over the decades.

The NDBI and NDVI are useful metrics calculated from Landsat 5 and 8 images on Google Earth Engine for examining land cover alterations. However, these constraints remain. The accuracy in metropolitan regions with mixed land cover may be impacted by the sensors' thirty-meter resolution, complicating the identification of urban variations. Where clouds regularly appear, the capacity to detect transient shifts is hampered by cloud cover.

ISSN: 2230-7990 (Online), ISSN: 2321-421X (Print)

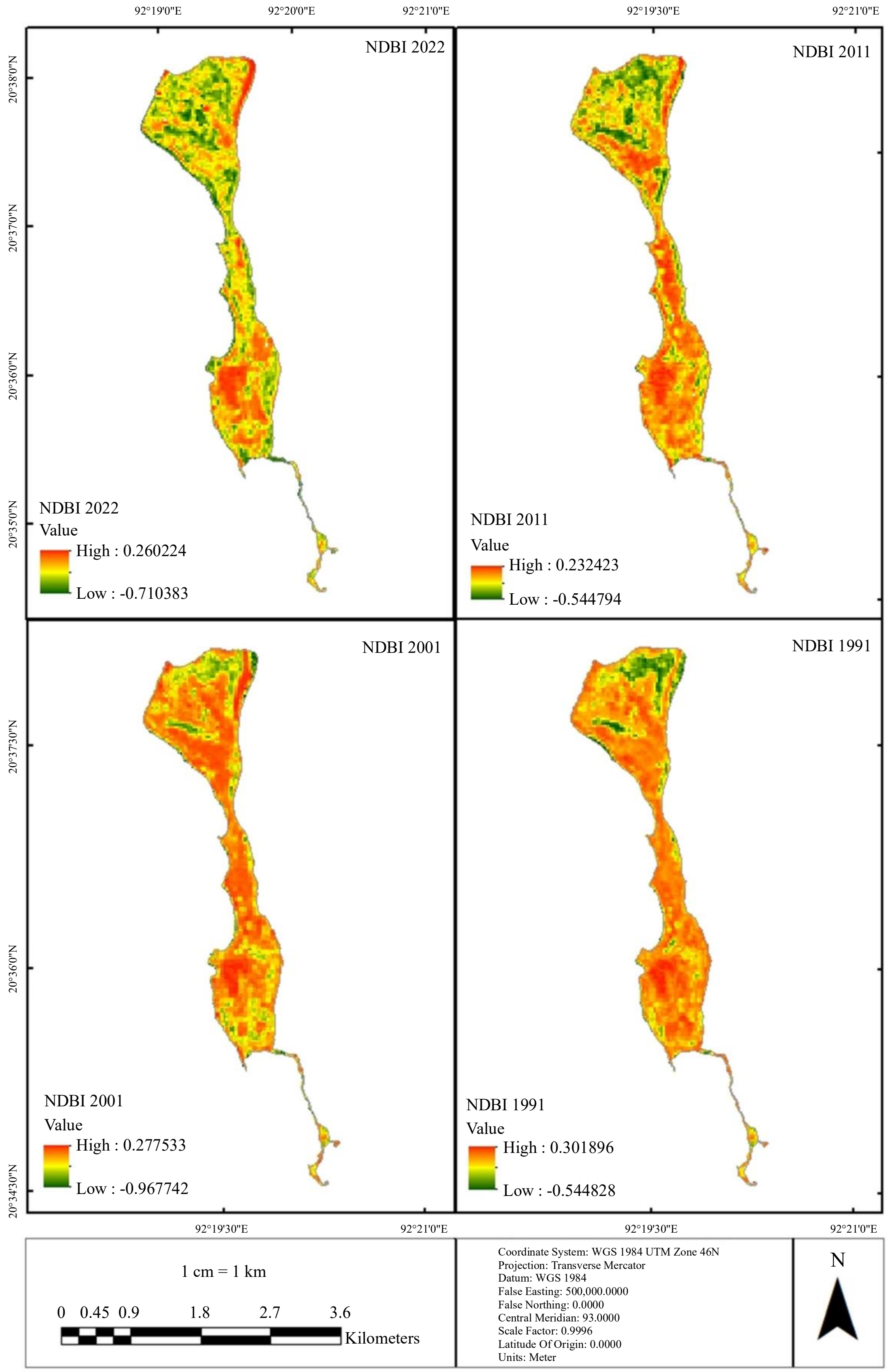

Figure 5. Represents NDBI of 1991, 2001, 2011, and 2022.

Table 2. Illustrate the NDVI-NDBI values of 1991, 2001, 2011, and 2022.

Indices	2022		2011		2001		1991	
	High	***Low***	***High***	***Low***	***High***	***Low***	***High***	***Low***
NDVI	0.872059	-0.505348	0.735107	-0.453629	0.749294	-0.509827	0.686572	-0.374884
NDBI	0.260224	-0.710383	0.232423	-0.544794	0.277533	-0.967742	0.301896	-0.544828

Compiled by Author 2023

The measurement precision of these indices can be affected by atmospheric conditions, such as clouds and airborne particles. Comparisons and a clear picture of vegetation proved difficult owing to sensor calibration variances and saturation effects in the biomass-rich regions. Misclassification risk exists in dynamic or rapidly shifting landscapes, resulting from shadows in hilly or urban spaces and the quality of training material defining classification accuracy. Additionally, the narrow spectral bands of Landsat 5 may reduce the distinguishing sharpness compared with Landsat 8. Researchers must understand and properly verify the outcomes within these boundaries, as Landsat imagery on GEE remains a strong instrument for large-scale land cover exploration.

Relationship Between NDVI-NDBI 1991, 2001, 2011, 2022

A complex JavaScript algorithm was used on the Google Earth Engine platform to precisely compute NDBI and NDVI at a granular level. An in-depth study was then carried out to determine the nuanced link between these two indices, with regression analysis employing sophisticated linear regression methods, shedding light on their intricate connections. Regression analysis plays a pivotal role in illuminating how subtle differences in land use intensity within heterogeneous land use and land cover units are expressed differently across different geographical landscapes. This analytical approach proved useful in disentangling the intra-land use variability of NDBI, a finding with significant implications. The following is a detailed examination of the full scope of the revelations yielded by this investigation. The correlations between NDVI-NDBI 1991, 2001, 2011, and 2022 are shown in Figure 6.

The negative correlation between NDVI and NDBI, evident in Figure 5, demonstrates a consistently weak relationship over the entire year. Specifically, the R2 values calculated for 1991, 2001, 2011, and 2022 correlations between NDVI and NDBI were 0.20, 0.44, 0.91, and 0.76, respectively. These statistical scatter plots provide a graphical representation of the values.

In 2022, the regression analysis graphs (Figure 6) revealed a somewhat negative linkage between vegetation and built-up indices, as evidenced herein. Conversely, between 1991-2011, a slight inverse, yet linear association existed between these indices. Consequently, NDBI can effectively showcase built-up area assessment and growth over time.

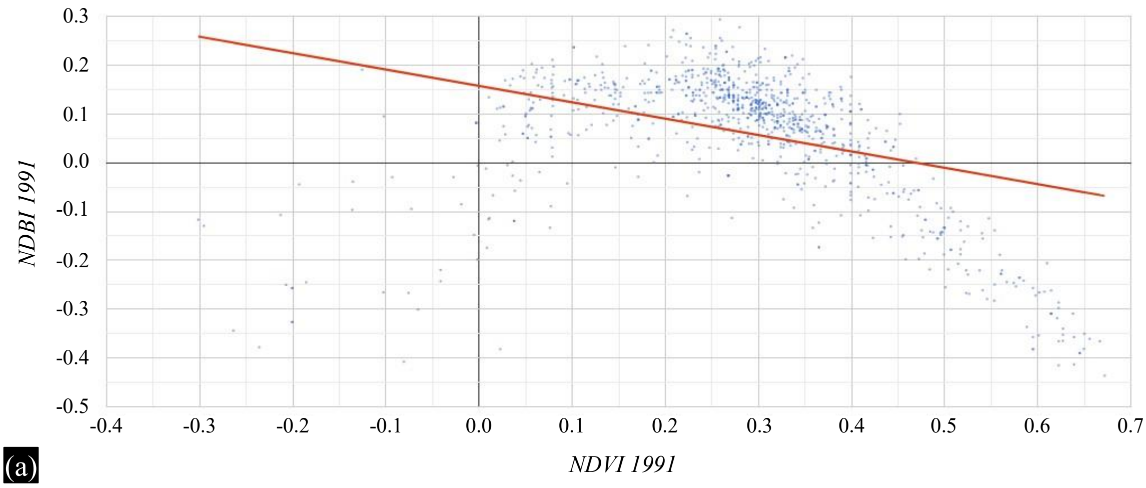

(a)

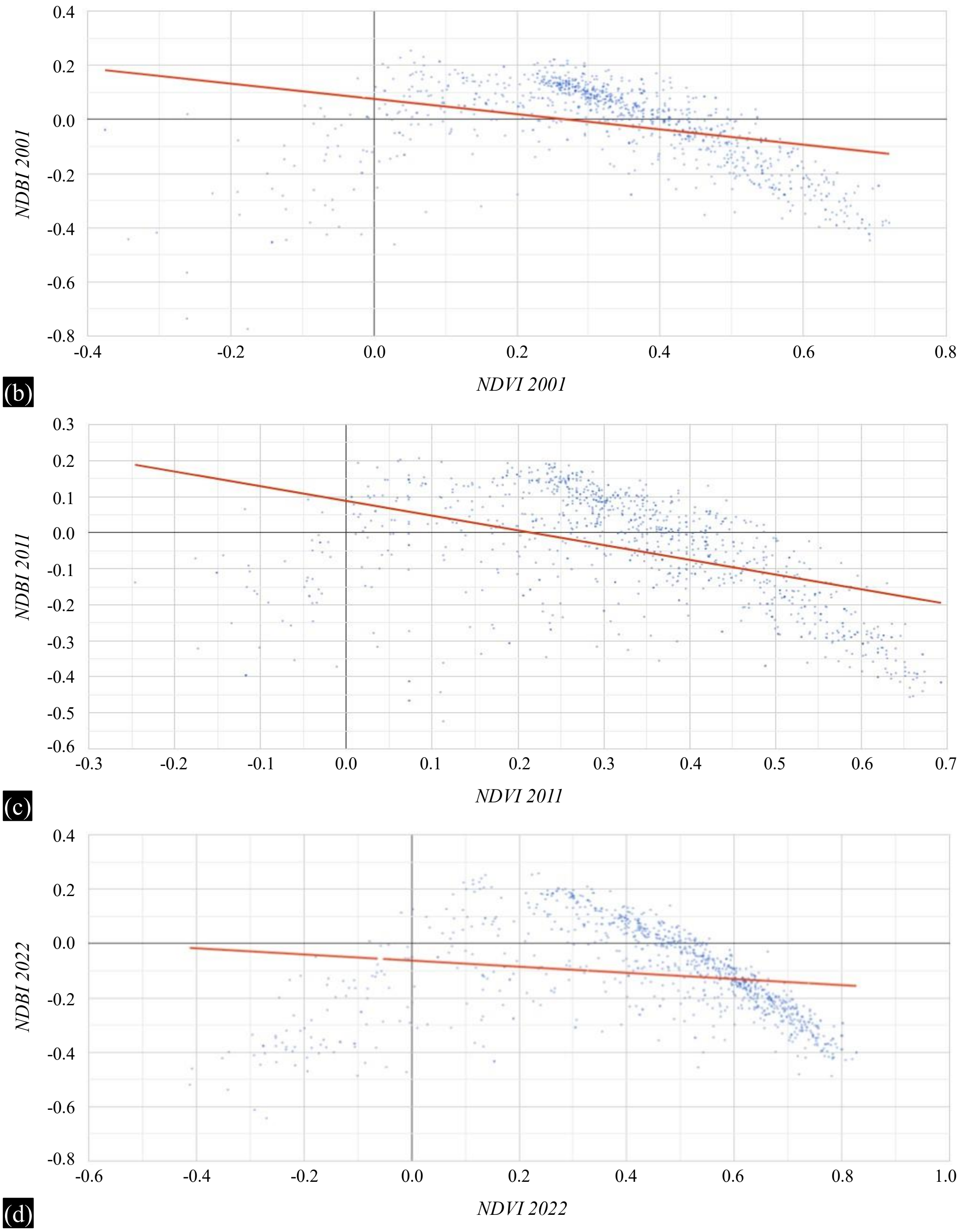

Figure 6. Represents the correlation between NDVI-NDBI 1991, 2001, 2011, and 2022.

The built-up presence minimally impacts the site vegetation volumes. Similarly, rising built environments accommodate regional tourism community expansion, permitting vegetation increase. Figure 6 clearly and concisely portrays the linear NDVI-NDBI connections across years via scatter plots.

Linear regression results indicated a somewhat negative 2022 correlation between built-up and vegetation areas, representing a limited rising interdependence. In contrast, from 1991 to 2011, there was little reliance on these variables. Both increased steadily throughout the study period. The current situation of the investigated region suggests that growing built-up regions exert some inverse vegetation influences, which are expected to intensify alongside additional settlements.

DISCUSSIONS

Globally, changes in land use have noticeably altered built-up areas through rapid urbanization, rising populations, intensifying industry, and burgeoning tourism in uninhabited areas. An amalgam of satellite imagery, surveys on location, and existing literature has evidenced that rapid demographic growth paired with haphazard urban development, widespread factories, and heightened commerce have discernibly impacted both plant life domains, such as farmlands, and broader environmental aspects. These impacts are shown in satellite photos.

The dynamics between land use and land cover display a broad spectrum of repercussions through indices connected to construction and vegetation. In one unique situation within the research, a meticulous computation of NDVI-NDBI patterns from 1991 through 2022 revealed a weak reverse link between the indices for vegetation and development. Consequently, we find value in participating in thorough debates and comparative analyses of results yielded by both indices during the pivotal years of 1991, 2001, 2011, and 2022. This investigation intends to provide an understanding of the intricate ties linking metropolitan growth and plant cover, along with their accumulated impact on shifting scenery across the local area under scrutiny. The NDVI readings across a decade fluctuated greatly, ranging in 1991 from dense vegetation, indicated by a mark of 0.686, to sparse or nonexistent greenery at -0.374. Lower scores commonly occur in locales, such as seas, barren terrain, and sandy spots; higher values often signify a thick canopy of flora, as is usual over forests and other heavily vegetated areas. By 2001, vegetation at its verdant peak had a high value of 0.749. In contrast, marks dipping as low as -0.509 principally appeared in domains with scarce or no plant life. Ten years later, in 2011, a peak NDVI of 0.735, generally spanning fertile fields and pastures, was documented. Conversely, sandy surfaces, long-abandoned villages, and desolate zones exhibited the lowest NDVI readings (-0.454). After a lengthy journey, the NDVI ultimately crested in 2022 at 0.872, dropping to -0.505. On the island of Saint Martin, these extremes manifest in beaches, urban centers, and rural areas. Examining the NDVI marks from 1991 to 2022, it is evident that botanical coverage increased considerably. 2022 boasted the highest NDVI, signifying an abundance of trees and lush agricultural land. In contrast, 1991 had the lowest NDVI, suggesting lower overall plant life. Consultations discovered that as human settlements swelled, farming also expanded, as gleaned from dialog with locals. Secondary data and expert perspectives noted a notable decrease in population density preceding the year 2000. A general upswing in vegetation resulted from a spike in tree planting and cultivation due to people flowing in for activities such as angling and tourism.

The NDBI values in 1991 ranged dramatically from 0.302, signifying substantial urban development, to -0.545, indicating locales with little to no constructed infrastructure. Higher scores were often correlated to places with dense populations and sparse vegetation, whereas lower values were observed in areas containing water bodies and abundant greenery. The year 2001 saw a peak NDBI of 0.278, indicating regions with considerable constructed buildings. In stark contrast, the bottom NDBI of -0.968 predominantly appeared in spots exhibiting minimal to no urban growth. The maximum NDBI recorded in 2011 was 0.232, specifically in human settlements, sandy terrain, and arid fields. In contrast, locales with the lowest NDBI values (-0.544) included regions with crops, greenery, and grasslands.

By 2022, NDBI peaked at 0.26 while reaching its nadir at -0.71. The existence of forest covers and waterways on Saint Martin Island is linked to these harsh conditions. Upon reviewing the pattern from 1991 to 2022, it is evident that there was an insignificant progression of constructed areas until 2011. A significant upsurge in urbanized regions materialized just before 2022, mostly owing to the prominent growth of tourism in the northern portion of the examined region. Additionally, it merits stating that some beaches underwent sediment deposition, where sand and rock were left by the ocean waters. The local observers witnessed this occurrence. This phenomenon may be ascribed to a variety of environmental factors that affect the dynamics of coastal regions. The examination focused on determining the bond between the NDVI and NDBI indices and exploring whether their ties were positive or negative. Data were gathered for 1991, 2001, 2011, and 2022. As evident in the scatterplots of Figure 5, a modest inverse link was visible throughout the years analyzed. The findings emphasize the minimal reciprocal sway between greenery and urban territories. Both tended to advance independently, with a steady upward pattern over time.

This may be ascribed to the diverse elements that shape the dynamics of these locales. According to fieldwork observations, travelers favored the northern section of the island, potentially clarifying its swifter growth than the south. Furthermore, the use of agricultural methods and tree planting has increased steadily. Ultimately, analysis of evidence, community perspectives, and supplemental sources all point to vegetation coverage exhibiting insignificant (or barely discernible) correlations with constructed regions. Supplementary studies and evaluations are necessary to better comprehend this design and formulate land use blueprints that facilitate potential future tourism growth. Given the island's history of tourism-driven progress, this could illuminate the intricate relationship between natural and man-made surroundings [14, 20–26].

CONCLUSIONS

From 1991 onwards, significant increases in both vegetation cover and built-up areas occurred, according to the research findings. Predominantly, the increase in vegetation cover seems to have developed separately without impacting the growth of urban regions based on the results. Natural processes are the primary drivers of this phenomenon, whereas human actions have minimal or insignificant influence. This suggests that urban and vegetated regions may be expanding at different paces, potentially owing to distinct natural and human-caused variables. Natural processes, such as reforestation, could be accountable for flourishing vegetation, whereas forces, including population growth and tourist development, may affect the extension of constructed areas. Further studies are required to better understand these dynamics and their underlying mechanisms.

Focusing on Saint Martin Island, this study generated NDVI and NDBI indices using Landsat 5 TM and Landsat 8 OLI/TIRS data throughout the chosen years. Consistently, regions with vegetation had decreased NDBI values, whereas towns, barren land, and sandy terrain showed increased values. The potential of NDVI and NDBI as robust indicators for monitoring vegetation, calculating agricultural acreage, and evaluating built-up urban zones is highlighted by the slightly negative connection found between the vegetation index and the built-up index from 1991 to 2022.

In summary, accurately mapping built-up regions in the study area using the built-up index is promising, especially with OLI/TIRS bands. Insights from this study could help the tourist industry to assess potential expansion patterns for a more environmentally friendly system. While it is critically important to continue growing the island's tourist industry, it is equally significant in that it does not disrupt the delicate ecological balance or diminish the quantity of plant cover. Additional studies on these indicators, particularly when combined with environmental characteristics, should be strongly encouraged by government organizations and legislators. Current land use patterns, especially in agricultural and urban settings, may be better understood with the aid of this expanded body of information. A broader scope of criteria, including landscape concerns, different ecosystem attributes, and the fast expansion of tourism, should be integrated into future research.

List of Abbreviations

GEE: Google Earth Engine
TM: Thematic Mapper
OLI: Operational Land Imager
TIRS: Thermal Infrared Sensor
NDVI: Normalized Difference Vegetation Index

NDBI: Normalized Difference Built-up Index
NDBal: Normalized Difference Bareness Index
BI: Bare Soil Index
UI: Urban Index
LST: Land Surface Index
FCC: False Color Composite
NIR: Near Infrared
MIR: Mid Infrared
SWIR: Shortwave Infrared

Declarations

Ethics approval and consent to participate

Not applicable. This study did not involve human participants, human data, or animals.

Consent for publication

The manuscript does not contain any individual data in any form (including individual details, images, or videos). Therefore, consent for publication was not applicable.

Availability of data and material

The data will be made available upon request from anyone.

Competing interests

The authors declare that they have no conflict of interest.

Funding

Not applicable.

Authors' Contributions

Md. Jakir Hossain conceived the study, designed the experiments, analyzed the data, and drafted the manuscript. Md. Munir Mahmud performed the experiments and helped draft the manuscript. Dr. Sheikh Tawhidul Islam provided essential documents and guidelines. All the authors have read and approved the final manuscript."

Acknowledgments

The authors would like to thank Dr. Sheikh Tawhidul Islam for her invaluable advice and insights on the manuscript. We also acknowledge the support of the Institute of Remote Sensing and GIS at Jahangirnagar University.

REFERENCES

1. Tan M. An intensity gradient/vegetation fractional coverage approach to mapping urban areas from dmsp/ols nighttime light data. IEEE J Sel Top Appl Earth Obs Remote Sens. 2017;10:95–103. doi:10.1109/JSTARS.2016.2566682.
2. Macarof P, Statescu F. Comparison of NDBI and NDVI as indicators of surface urban heat island effect in Landsat 8 imagery: A case study of Iasi. Present Environ Sustain Dev. 2017;11:141–50. doi:10.1515/pesd-2017-0032.
3. Tania TC. Socio-economic culture and tourism: A case study on Saint Martin Island of Bangladesh. J Apl Manaj Ekon Bisnis. 2024;6:84–93. doi:10.51263/jameb.v6i2.148.
4. Sobhani B, Abad B, Kefayat Motlagh OM. Identification of vegetation coverage seasons in Iran using enhanced vegetation index (Evi). Appl Ecol Environ Res. 2018;16:3861–72. doi:10.15666/aeer/1604_38613872.
5. Islam MM, Mamun MMI. Variations of NDVI and Its Association with Rainfall and Evapotranspiration over Bangladesh. Rajshahi Univ J Sci Eng. 2015;43:21–8. doi:10.3329/rujse.v43i0.26160.

6. Pamungkas S. Analysis of vegetation index for NDVI, EVI-2, and savi for mangrove forest density using Google Earth Engine in Lembar Bay, Lombok Island. IOP Conf Ser Earth Environ Sci. 2023;1127:012034. doi:10.1088/1755-1315/1127/1/012034.
7. Arias ME, Celemín JP. Distribución espacial del arbolado viario en el centro de la ciudad de Santiago del Estero (Argentina). Rev Casa Geogr Sobral. 2021;23:434–54. doi:10.35701/rcgs.v23.811.
8. Paul SI, Rahman MM, Salam MA, Khan MAR, Islam MT. Identification of marine sponge-associated bacteria of the Saint Martin’s island of the Bay of Bengal emphasizing on the prevention of motile Aeromonas septicemia in Labeo rohita. Aquaculture. 2021;545:737156. doi:10.1016/j.aquaculture.2021.737156.
9. Ghose T, Hossain M. Socioeconomic factors affecting profitability of seaweed culture in Saint Martin Island of Bangladesh. Prog Agric. 2021;31:227–34. doi:10.3329/pa.v31i3.52127.
10. Hossain F, Akter S, Ahsan A. Digital elevation modeling of Saint Martin Island, Bangladesh: A method based on open source Google Earth data. Int J Adv Res. 2018 Feb;6(2):379–89. doi:10.21474/IJAR01/6449.
11. Alam O, Deng T, Uddin M, Alamgir M. Application of environmental ethics for sustainable development and conservation of Saint Martins Island in Bangladesh. J Environ Sci Nat Resour. 2015;8:19–27. doi:10.3329/jesnr.v8i1.24628.
12. Gazi MY, Mowsumi TJ, Ahmed MK. Detection of coral reefs degradation using geospatial techniques around Saint Martin’s Island, Bay of Bengal. Ocean Sci J. 2020;55:419–31. doi:10.1007/s12601-020-0029-3.
13. Li G, Lu D, Moran E, Hetrick S. Mapping impervious surface area in the Brazilian Amazon using Landsat Imagery. GISci Remote Sens. 2013;50:172–83. doi:10.1080/15481603.2013.780452.
14. Lipu MSH, Golam Haz M, Ullah MS, Hossain A, Munia FY. Design optimization and sensitivity analysis of hybrid renewable energy systems: A case of Saint Martin Island in Bangladesh. Int J Renew Energy Res. 2017;v7i2. doi:10.20508/ijrer.v7i2.5762.g7079.
15. Hossain MJ, Mahmud MM, Islam ST. Monitoring spatiotemporal changes of urban surface water based on satellite imagery and Google Earth Engine platform in Dhaka City from 1990 to 2021. Bull Natl Res Cent. 2023;47:150. doi:10.1186/s42269-023-01127-5.
16. Rahaman SN, Shermin N. Identifying the effect of monsoon floods on vegetation and land surface temperature by using Google Earth Engine. Urban Clim. 2022;43:101162. doi:10.1016/j.uclim.2022.101162.
17. Guha S, Govil H. A seasonal relationship between land surface temperature and normalized difference bareness index. S Afr J Geomat. 2022;10:163–80. doi:10.4314/sajg.v10i2.12.
18. Kong D, Zhang Y, Gu X, Wang D. A robust method for reconstructing global MODIS EVI time series on the Google Earth Engine. ISPRS J Photogramm Remote Sens. 2019;155:13–24. doi:10.1016/j.isprsjprs.2019.06.014.
19. Keerthi Naidu BN, Chundeli FA. Assessing LULC changes and LST through NDVI and NDBI spatial indicators: A case of Bengaluru, India. GeoJournal. 2023;88:4335–50. doi:10.1007/s10708-023-10862-1.
20. Sultana S, Islam M, Arabi SZ. Coexistence of wildlife with modern tourism: The context of Bangladesh. Bus Manag Rev. 2020;11:64–8. doi:10.24052/BMR/V11NU02/ART-08.
21. Ali Shah S, Kiran M, Nazir A, Ashrafani SH. Exploring NDVI and NDBI relationship using Landsat 8 OLI/TIRS in Khangarh Taluka, Ghotki. Malays J Geosci. 2022;6:8–11. doi:10.26480/mjg.01.2022.08.11.
22. Eswar R, Sekhar M, Bhattacharya BK. Disaggregation of LST over India: Comparative analysis of different vegetation indices. Int J Remote Sens. 2016;37:1035–54. doi:10.1080/01431161.2016.1145363.
23. Guha S, Govil H. Land surface temperature and normalized difference vegetation index relationship: A seasonal study on a tropical city. SN Appl Sci. 2020;2:1661. doi:10.1007/s42452-020-03458-8.
24. Hossen MF, Sultana N. Shoreline change detection using DSAS technique: Case of Saint Martin Island, Bangladesh. Remote Sens Appl Soc Environ. 2023;30:100943. doi:10.1016/j.rsase.2023.100943.

25. Kulkarni K, Vijaya P. NDBI based prediction of land use land cover change. J Indian Soc Remote Sens. 2021;49:2523–37. doi:10.1007/s12524-021-01411-9.
26. Vollmar M, Rasi R, Beuchle R, Simonetti D, Stibig HJ, Achard F. Combining Landsat TM/ETM+ and ALOS AVNIR-2 satellite data for tropical forest cover change detection. IEEE J Sel Top Appl Earth Obs Remote Sens. 2013;6:102–9. doi:10.1109/JSTARS.2013.2241017.

APPENDIX

JavaScript Code for Geospatial Analysis of satellite images:

NDVI-NDBI-Correlation * Get Link Save Run Reset Apps

```
Imports (1 entry)
var roi: Table users/jakirhossainurpju45/SaintMartin_AOI

// Import the Landsat 5/8 image collection.
//var l8 = ee.ImageCollection('LANDSAT/LC08/C02/T1_TOA');

//var l5 = ee.ImageCollection('LANDSAT/LT05/C01/T1_SR')
var l8 = ee.ImageCollection('LANDSAT/LC08/C01/T1_SR')

// Get the least cloudy image.
var image = ee.Image(
  l8.filterBounds(roi)
    .filterDate('2022-01-01', '20222-03-31')
    .sort('CLOUD_COVER')
    .first()
    .clip(roi)
);
print(image)

// Compute the Normalized Difference Vegetation Index (NDVI).
var nir = image.select('B5');
var red = image.select('B4');
var ndvi = nir.subtract(red).divide(nir.add(red)).rename('NDVI');
//var ndvi = image.normalizedDifference(['B5', 'B4']).rename('NDVI');

// Display the result.
Map.centerObject(ndvi, 12);
var ndviParams = {min: -1, max: 1, palette: ['blue', 'white', 'green']};
Map.addLayer(ndvi, ndviParams, 'NDVI');

// Compute the Normalized Difference Built-up Index (NDBI).
var b6 = image.select('B6');
var b5 = image.select('B5');
var ndbi = b6.subtract(b5).divide(b6.add(b5)).rename('NDBI');

// Display the result.
Map.centerObject(ndvi, 12)
```

NDVI-NDBI-Correlation * Get Link Save Run Reset Apps

```
// Display the result.
Map.centerObject(ndvi, 12)
var ndbiParams = {min: -1, max: +1, palette:['red','yellow','green']};
Map.addLayer(ndbi, ndbiParams, 'NDBI');

// Display the result.
var visPaaramsTrue = {bands: ['B3', 'B2', 'B1'], min: 0, max:3000, gamma: 1.4};
Map.addLayer(image, visPaaramsTrue, 'Landsat Image',false);

// Export to Drive
Export.image.toDrive({
  image: ndvi.clip(roi),
  description: 'NDVI1991',
  folder: 'GEE_Export',
  scale: 12,
  region: roi,
  //maxPixels: 1e13
});

// Export to Drive
Export.image.toDrive({
  image: ndbi.clip(roi),
  description: 'NDBI1991',
  folder: 'GEE_Export',
  scale: 12,
  region: roi,
  //maxPixels: 1e13
});

 // Get the intersection between the two images - the area of interest (aoi).
var aoi2 = ndvi.geometry().intersection(ndbi.geometry());

// Create 1000 random points in the region.
var randomPoints = ee.FeatureCollection.randomPoints(roi);

// Display the points.
Map.centerObject(randomPoints);
Map.addLayer(randomPoints, {}, 'random points');
```

NDVI-NDBI-Correlation * Get Link Save Run Reset Apps

```

// Display the points.
Map.centerObject(randomPoints);
Map.addLayer(randomPoints, {}, 'random points');

// Combine the SWIR1 bands from each image into a single image.
var combo = ndvi.select('NDVI')
  .addBands(ndbi.select('NDBI'))
  .rename(['ndvi', 'ndbi']);

// Sample the SWIR1 bands using the sample point feature collection.
var imgSamp = combo.sampleRegions({
  collection: randomPoints,
  scale: 30
})
// Add a constant property to each feature to be used as an independent variable.
.map(function(feature) {
  return feature.set('constant', 1);
});

// Compute linear regression coefficients.
var linearRegression = ee.Dictionary(imgSamp.reduceColumns({
  reducer: ee.Reducer.linearRegression({
    numX: 2,
    numY: 1
  }),
  selectors: ['constant', 'ndvi', 'ndbi']
}));

// Convert the coefficients array to a list.
var coefList = ee.Array(linearRegression.get('coefficients')).toList();

// Extract the y-intercept and slope.
var yInt = ee.List(coefList.get(0)).get(0); // y-intercept
var slope = ee.List(coefList.get(1)).get(0); // slope

// Gather the values from the point sample into a list of lists.
var props = ee.List(['ndvi', 'ndbi']);
```

NDVI-NDBI-Correlation * Get Link Save Run Reset Apps

```
// Gather the values from the point sample into a list of lists.
var props = ee.List(['ndvi', 'ndbi']);
var regressionVarsList = ee.List(imgSamp.reduceColumns({
  reducer: ee.Reducer.toList().repeat(props.size()),
  selectors: props
}).get('list'));

var x = ee.Array(ee.List(regressionVarsList.get(0)));
var y1 = ee.Array(ee.List(regressionVarsList.get(1)));

var y2 = ee.Array(ee.List(regressionVarsList.get(0)).map(function(x) {
  var y = ee.Number(x).multiply(slope).add(yInt);
  return y;
}));

var yArr = ee.Array.cat([y1, y2], 1);

print(ui.Chart.array.values({
  array: yArr,
  axis: 0,
  xLabels: x})
  .setChartType('ScatterChart')
  .setOptions({
    legend: {position: 'none'},
    hAxis: {'title': 'NDVI 2022'},
    vAxis: {'title': 'NDBI 2022'},
    series: {
      0: {
        pointSize: 0.2,
        dataOpacity: 0.5,
      },
      1: {
        pointSize: 0,
        lineWidth: 2,
      }
    }
  })
);
```

ISSN: 2230-7990 (Online), ISSN: 2321-421X (Print)

Output 01

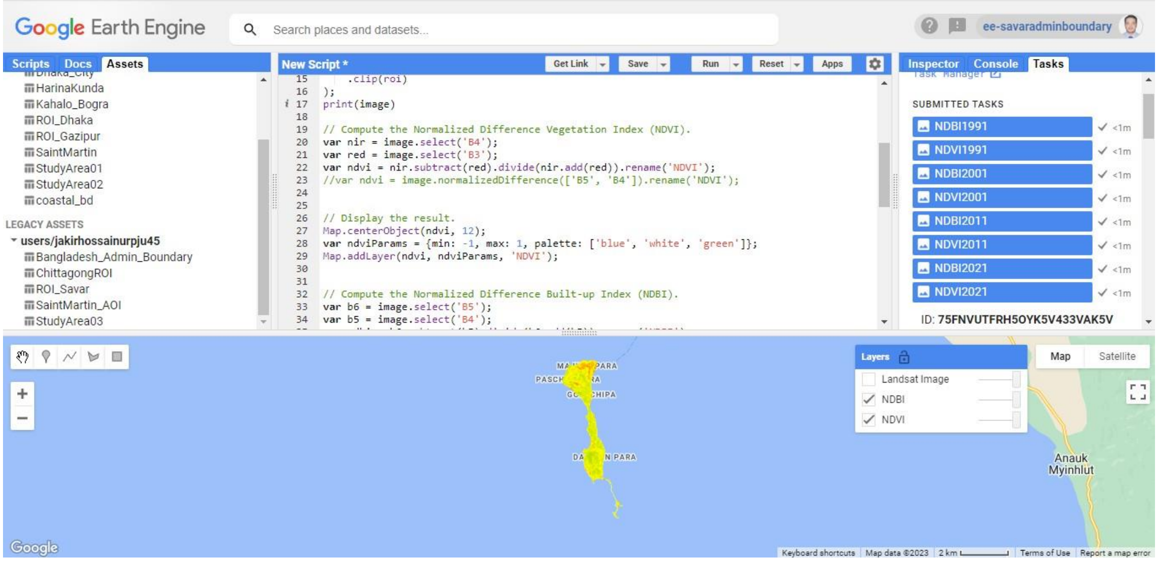

Output 02